

# Symmetry-breaking for a restricted $n$ -body problem in the Maxwell-ring configuration

Renato Calleja<sup>1,a</sup>, Eusebius Doedel<sup>2,b</sup>, and Carlos García-Azpeitia<sup>3,c</sup>

<sup>1</sup> Matemáticas y Mecánica, IIMAS, Universidad Nacional Autónoma de México, Admon. No. 20, Delegación Alvaro Obregón, 01000 México D.F.

<sup>2</sup> Department of Computer Science, Concordia University, 1455 boulevard de Maisonneuve O., Montréal, Québec H3G 1M8, Canada

<sup>3</sup> Departamento de Matemáticas, Facultad de Ciencias, Universidad Nacional Autónoma de México, 04510 México DF, Mexico

**Abstract.** We investigate the motion of a massless body interacting with the Maxwell relative equilibrium, which consists of  $n$  bodies of equal mass at the vertices of a regular polygon that rotates around a central mass. The massless body has three equilibrium  $\mathbb{Z}_n$ -orbits from which families of Lyapunov orbits emerge. Numerical continuation of these families using a boundary value formulation is used to construct the bifurcation diagram for the case  $n = 7$ , also including some secondary and tertiary bifurcating families. We observe symmetry-breaking bifurcations in this system, as well as certain period-doubling bifurcations.

## Introduction

In his 1859 essay [9] Maxwell proposed a model to study the rings of Saturn. His model consists of  $n$  bodies of equal mass at the vertices of a regular polygon that rotates around a massive body at the center. Maxwell used Fourier analysis and dispersion relations in the determination of the stability of the ring. The Maxwell equilibrium has been studied in several papers since then. In particular, Moeckel proved in [10] that the equilibrium is stable if  $n \geq 7$  and the body at the center massive enough. See also [4,11,13] and references therein.

In this paper we consider the motion of a satellite under the gravitational effect of the Maxwell equilibrium. Several papers have been devoted to study the stability and bifurcation of periodic solutions for the restricted  $N$ -body problem in the Maxwell configuration. For example, a study of the existence and linear stability of equilibrium positions can be found in [1], an analysis of the bifurcation of planar and vertical families of periodic solutions in [3], and a numerical exploration in [6].

Given that a change of stability occurs at  $\mu_1 \approx 584$  when  $n = 7$ , we present a numerical exploration of the motion of the satellite for this stable system, taking

---

<sup>a</sup> e-mail: calleja@mym.iimas.unam.mx

<sup>b</sup> e-mail: doedel@cs.concordia.ca

<sup>c</sup> e-mail: cgazpe@ciencias.unam.mx

$\mu = 10^3$ . We follow the planar and vertical Lyapunov families that were proved to exist in [3], and we compute new, secondary families that bifurcate from the Lyapunov families. These numerical results allow us to construct a bifurcation diagram in Figure 2 that shows primary, secondary, and tertiary bifurcating families. The results also allow us to present the isotropy lattice in Figure 3 which shows the symmetries of these families.

The numerical computations in this paper are done using continuation methods and boundary value techniques for determining the periodic orbits that emanate from the equilibrium orbits. Python scripts that make the AUTO software perform the calculations reported in this paper will be made freely available. Similar techniques have been applied to the restricted 3-body problem; see for example [14], where a detailed bifurcation diagram with various families of periodic orbits can be found.

This paper is organized as follows. In Section 1 we recall some key results from the literature concerning the equilibria and the Lyapunov orbits of the problem. In Section 2 we present a bifurcation diagram and an isotropy lattice for the restricted  $N$ -body problem in the Maxwell configuration, with  $n = 7$  and  $\mu = 10^3$ . In Section 3 we describe the isotropy groups of the Lyapunov families. In Section 4 we address secondary bifurcations, and in Section 5 describe some tertiary families. We also present evidence of the existence of invariant tori foliated by periodic orbits. Finally, in Section 6, we consider the breaking of symmetries of planar interplanetary periodic orbits.

## 1 The restricted $N$ -body problem

The Maxwell relative equilibrium consists of a body of mass  $\mu$  at  $\mathbf{a}_0 = \mathbf{0} \in \mathbb{R}^3$ , and  $n$  bodies of mass 1 located at  $\mathbf{a}_j = (e^{ij\zeta}, 0) \in \mathbb{R}^3$ ,  $j = 1, \dots, n$ , where  $\zeta = 2\pi/n$ . These positions and masses correspond to a relative equilibrium solution of Newton's equations,  $\mathbf{q}_j(t) = e^{\mathcal{J}t}\mathbf{a}_j$ , when the masses are renormalized by  $\mu + s$  [1,3], where  $\mathcal{J} = \text{diag}(J, 0)$ ,

$$J = \begin{pmatrix} 0 & -1 \\ 1 & 0 \end{pmatrix}, \quad s = \frac{1}{4} \sum_{j=1}^{n-1} \frac{1}{\sin(j\pi/n)}.$$

The equation of a satellite in rotating coordinates,  $\mathbf{q}(t) = e^{\mathcal{J}t}\mathbf{u}$ , is

$$\ddot{\mathbf{u}} + 2\mathcal{J}\dot{\mathbf{u}} = \nabla V, \quad (1)$$

where  $\mathbf{u} = (x, y, z) \in \mathbb{R}^3$  and

$$V(\mathbf{u}) = \frac{1}{2} \|(x, y)\|^2 + \frac{\mu}{s + \mu} \frac{1}{\|\mathbf{u}\|} + \sum_{j=1}^n \frac{1}{s + \mu} \frac{1}{\|\mathbf{u} - (e^{ij\zeta}, 0)\|}. \quad (2)$$

The first term of the potential  $V(\mathbf{u})$  in Equation (2) corresponds to the centrifugal force, the second term is the interaction with the mass  $\mu$ , and the third term models the interaction with the  $n$  primaries of mass 1; see [1] and [3]. The equilibrium positions of the satellite are critical points of  $V$ , defined in Equation (2). Moreover, due to the particular form of the Maxwell configuration, the potential  $V$  is  $\mathbb{Z}_n$ -invariant. In this respect the existence of three  $\mathbb{Z}_n$  equilibrium orbits for any value of  $\mu$  is proved in [1,3]. For small  $\mu$ , two additional equilibrium orbits appear close to the origin [3]; see Figure 1.

In [3], taking advantage of the symmetries of the equations, the authors analyze the bifurcation of periodic solutions from the  $\mathbb{Z}_n$ -orbits of equilibria. Here we state these results for the equilibria  $\mathcal{L}_1$ ,  $\mathcal{L}_2$  and  $\mathcal{L}_3$  of the three  $\mathbb{Z}_n$ -orbits:

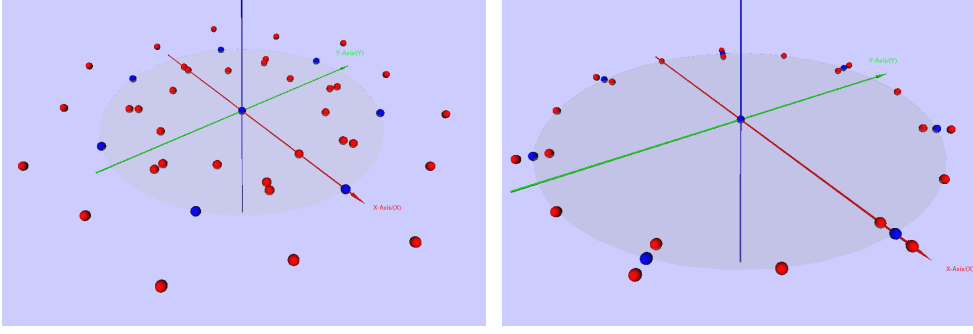


**Fig. 1.** The Maxwell configuration with the masses colored blue and the equilibrium orbits colored red. Left: the 35 equilibria when  $\mu = 3$ . Right: the 21 equilibria when  $\mu = 1000$ .

**Theorem 1** [Ize & García-Azpeitia [3].] *The libration point  $\mathcal{L}_1$ , has one global bifurcation family of planar periodic solutions that will be denoted by  $L_1$ , and one global family of vertical solutions, denoted by  $V_1$ . Similarly, the libration point  $\mathcal{L}_2$  has one global family of planar periodic solutions, denoted  $L_2$ , and one family of vertical solutions,  $V_2$ . For  $\mu > \mu_1$ , the equilibrium  $\mathcal{L}_3$  has two global bifurcations of planar solutions, one of which has longer period, denoted  $L_{3l}$ , and another planar family of shorter period,  $L_{3s}$ . There is also a bifurcating family of vertical periodic solutions that will be denoted by  $V_3$ . Moreover, as a consequence of the symmetries, the shape of all vertical solutions close to the equilibrium resembles a spatial figure eight.*

The *global* property guarantees that the family is a continuum that either goes to infinity in Sobolev norm or period, ends in a collision, or ends at a bifurcation point. Indeed, each one of these possibilities appears in the numerical continuation of the families, as illustrated in the bifurcation diagram in Figure 2.

## 2 Breaking of symmetries

In this section we discuss the breaking of symmetries of Equation (1) for the case  $n = 7$  and  $\mu = 10^3$ , as observed in the numerically computed Lyapunov families that emerge from the libration points and the secondary families that bifurcate from them.

The  $2\pi/\nu$ -periodic solutions of Equation (1) are zeros of the map

$$\mathbf{f}(\mathbf{u}; \nu) = \nu^2 \ddot{\mathbf{u}} + \mathcal{J} \nu \dot{\mathbf{u}} - \nabla V(\mathbf{u}),$$

defined in a set of  $2\pi$ -periodic collisionless functions  $\mathbf{u}$ ; see [3]. Since the potential is  $\mathbb{Z}_7$ -invariant and the equations are autonomous, the map  $\mathbf{f}$  is equivariant under the action of  $(\zeta, \varphi) \in \mathbb{Z}_7 \times S^1$  given by

$$\rho(\zeta, \varphi)\mathbf{u}(t) = e^{\mathcal{J}\zeta} \mathbf{u}(t + \varphi),$$

where  $\zeta = 2\pi/7$ . In addition the equations are symmetric with respect to reflection of  $y$  about the  $xz$  plane, while reversing time, and with respect to reflection of  $z$  about the  $xy$  plane. In this regard we define the reflections  $\kappa_y$  and  $\kappa_z$  by

$$\rho(\kappa_y)\mathbf{u}(t) = R_y \mathbf{u}(-t) \quad \text{and} \quad \rho(\kappa_z)\mathbf{u}(t) = R_z \mathbf{u}(t),$$

where  $R_y = \text{diag}(1, -1, 1)$  and  $R_z = \text{diag}(1, 1, -1)$ . Therefore the map  $\mathbf{f}$  is equivariant under the full symmetry group

$$G = (\mathbb{Z}_7 \times S^1 \cup \kappa_y(\mathbb{Z}_7 \times S^1)) \times \mathbb{Z}_2(\kappa_z). \quad (3)$$

We will use the property that the group orbit of a function  $\mathbf{u}$ ,

$$G(\mathbf{u}) = \{\rho(\gamma)\mathbf{u} : \gamma \in G\},$$

is isomorphic to  $G/G_{\mathbf{u}}$ , where  $G_{\mathbf{u}}$  is the isotropy group defined as

$$G_{\mathbf{u}} = \{\mathbf{u} : \rho(\gamma)\mathbf{u} = \mathbf{u}, \forall \gamma \in G\}.$$

In this sense the libration equilibria  $\mathcal{L}_j$ , for  $j = 1, 2, 3$ , have group orbits  $G(\mathcal{L}_j) \simeq \mathbb{Z}_7$  and isotropy group

$$G_{\mathcal{L}_j} = (S^1 \cup \kappa_y S^1) \times \mathbb{Z}_2(\kappa_z).$$

We therefore present the breaking of symmetries only for the libration points  $\mathcal{L}_j$ ,  $j = 1, 2, 3$ .

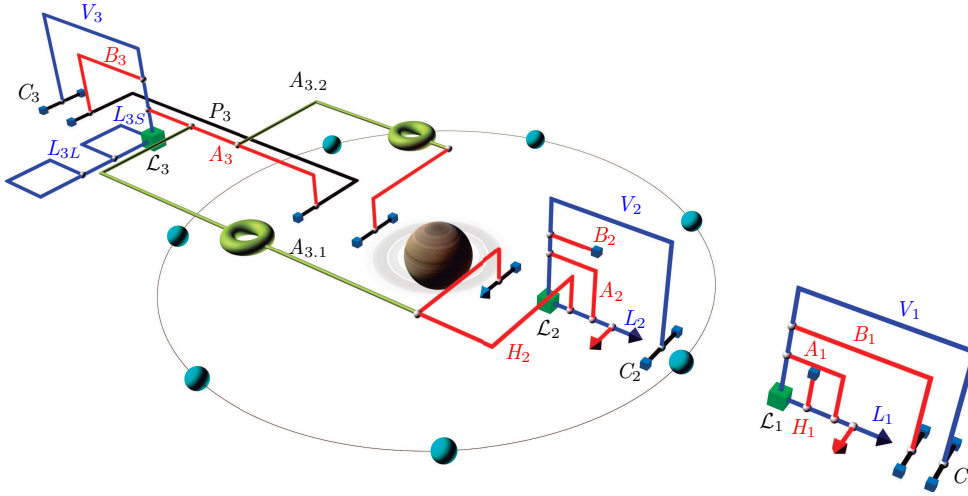


**Fig. 2.** Bifurcation diagram for  $\mu = 10^3$ : The green cubes denote the equilibrium positions  $\mathcal{L}_1$ ,  $\mathcal{L}_2$ , and  $\mathcal{L}_3$ , the white spheres represent bifurcation points, the blue cubes represent families that apparently end in collisions, and tetrahedra indicate that the family goes to infinity in period or in Sobolev norm.

The bifurcation diagram for the case  $\mu = 10^3$  is given in Figure 2. The blue lines represent the vertical Lyapunov families  $V_j$  and the planar Lyapunov families  $L_j$ ,  $j = 1, 2, 3$ . Planar families are positioned in the plane of the bodies, as are the black lines that represent planar interplanetary orbits. The red lines are the result of a secondary symmetry-breaking, with two solutions per equilibrium, as for the Halo orbits  $H_j$  and the Axial orbits  $A_j$ ,  $j = 1, 2, 3$ . The green lines correspond to a tertiary symmetry-breaking, and as such they have a trivial isotropy group and four symmetry-related branches per libration point.

*Remark 1* : Some of the families in the bifurcation diagram that end at a tetrahedron, in fact terminate as a heteroclinic orbit. For the restricted three-body problem similar heteroclinic orbits are given in [2,8], and the existence of heteroclinic connections is proved in [7]. In future work we will present many other heteroclinic connections that we have located by continuation of orbits in stable/unstable manifolds. Furthermore, in future work we will present evidence of families of planar orbits that interconnect



the planar families  $L_{3s}$  and  $L_{3l}$ , as in [5]. All results are accompanied by scripts that allow their reproduction.

The breaking of symmetries in the bifurcation diagram gives rise to the isotropy lattice in Figure 3.

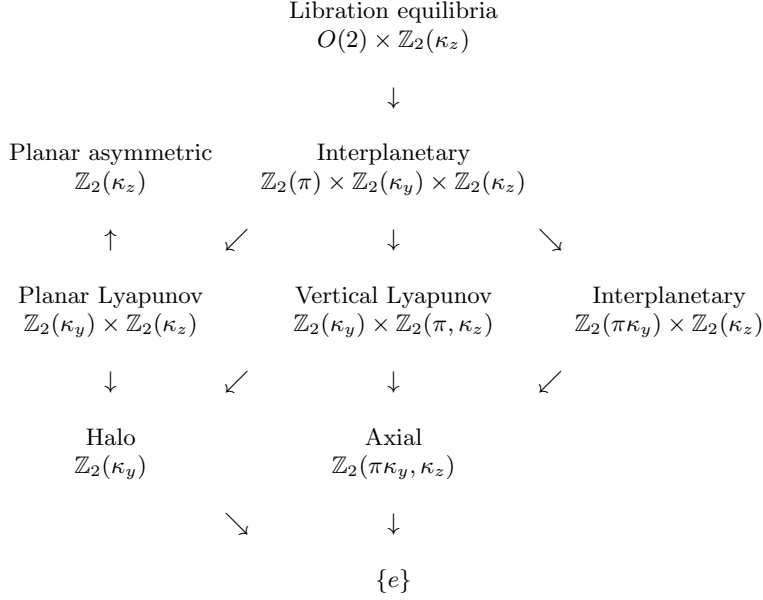


**Fig. 3.** Isotropy lattice

### 3 Lyapunov families

The first bifurcation occurs when the  $S^1$ -symmetry is broken, giving rise to the Lyapunov families (the blue lines in Figure 2) from the equilibria  $\mathcal{L}_j$ ,  $j = 1, 2, 3$ . The number of symmetry-related Lyapunov branches is equal to the order of  $G/G_{\mathbf{u}}$ , which is 7, since each isotropy group is isomorphic to  $\mathbb{Z}_2 \times \mathbb{Z}_2$ .

The isotropy group of the planar Lyapunov orbits that emerge from the libration equilibria is

$$G_{L_j} = \mathbb{Z}_2(\kappa_y) \times \mathbb{Z}_2(\kappa_z) < G_{\mathcal{L}_j}. \quad (4)$$

These periodic solutions have the property that  $x(t)$  is even,  $y(t)$  is odd, and  $z(t) = 0$ . In particular, we observe that the planar orbits are invariant under the transformation that takes  $y$  to  $-y$ .

For the vertical Lyapunov orbits the isotropy group is

$$G_{V_j} = \mathbb{Z}_2(\kappa_y) \times \mathbb{Z}_2(\pi, \kappa_z) < G_{\mathcal{L}_j}. \quad (5)$$

Here a solution is fixed by  $G_{V_j}$  if it satisfies

$$\mathbf{u}(t) = \rho(\kappa, \pi)\mathbf{u}(t) = R_z\mathbf{u}(t + \pi),$$

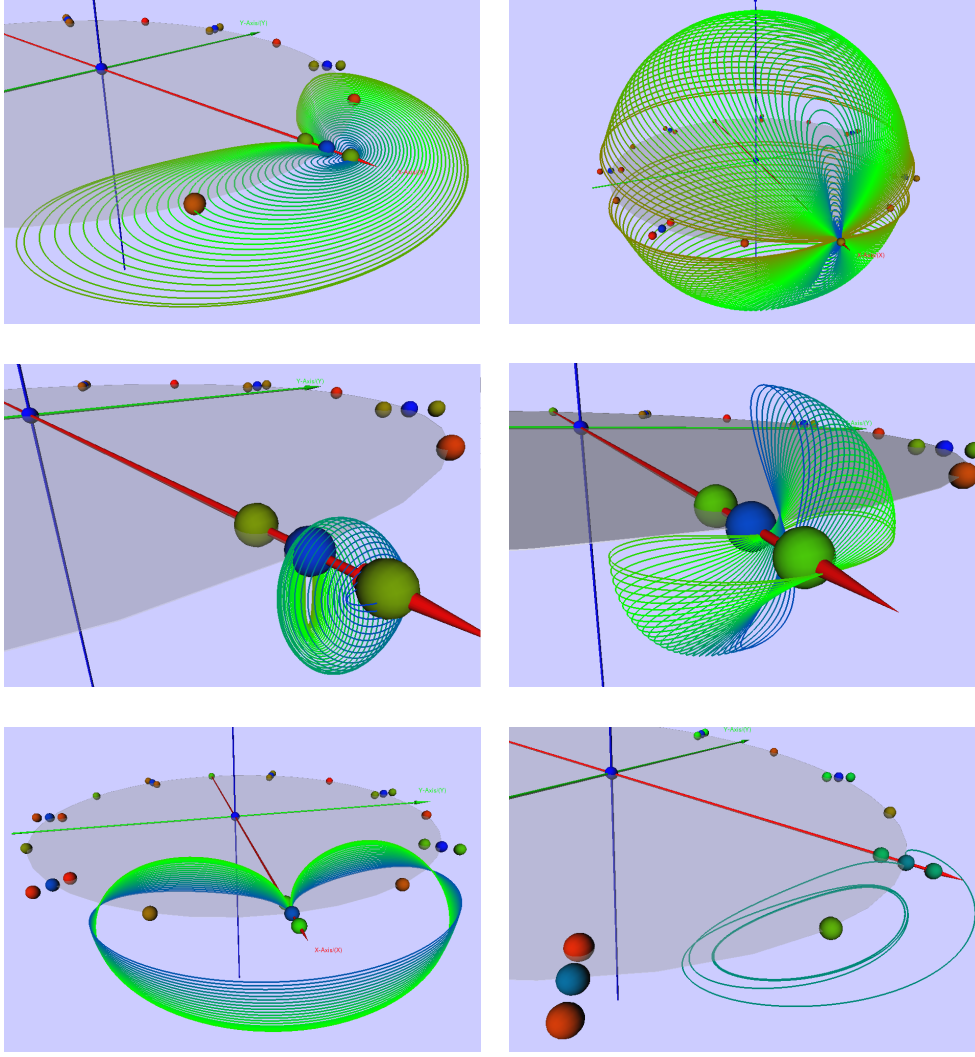


**Fig. 4.** Top Left: The planar Lyapunov family  $L_1$ , which ends in a collision orbit. Top Right: The vertical family  $V_1$  until its second bifurcation orbit. Center Left: The “Southern” branch of the Halo family  $H_1$ , which ends in a collision orbit. Center Right: One branch of the Axial family  $A_1$ , which forms a “bridge” between  $L_1$  and  $V_1$ . Bottom Left: One branch of the third family that bifurcates from  $L_1$ , which ends in a collision orbit. Bottom Right: One branch of the fourth family that bifurcates from  $L_1$ , which approaches an orbit that is homoclinic to a periodic orbit.

which is equivalent to assuming that  $x(t)$  is a  $\pi$ -periodic even function,  $y(t)$  is a  $\pi$ -periodic odd function, and  $z(t) = -z(t + \pi)$ . Therefore these solutions follow the planar  $\pi$ -periodic curve  $(x, y)$  twice; one time with the spatial coordinate  $z$  and a second time with  $-z$ . This fact was proved in [3].

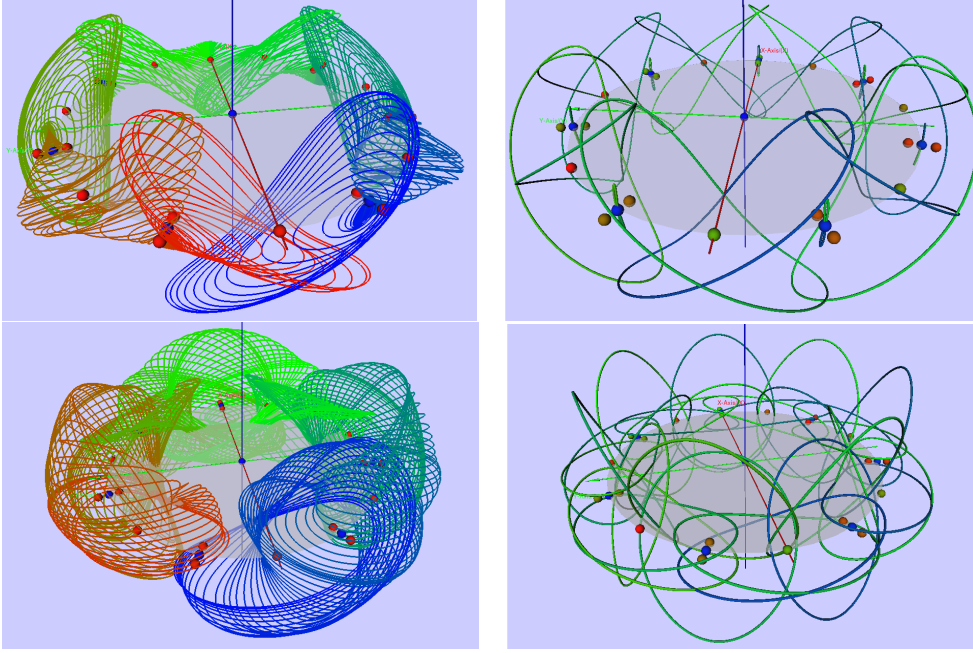


**Fig. 5.** Top Left: Part of the torus generated by the family  $A_{3,1}$ ; the torus closes up after making two full rounds. Top Right: Bifurcation orbits along the torus generated by  $A_{3,1}$ . Bottom Left: Part of the torus generated by the family  $A_{3,2}$ ; This torus also closes up after making two full rounds. Bottom Right: Bifurcation orbits along the torus generated by  $A_{3,2}$ .

## 4 Secondary families

The bifurcations from the Lyapunov families coincide with the second breaking of symmetries. The families that emanate from such bifurcation points (the red lines in Figure 2) have three kinds of isotropy groups, each one isomorphic to  $\mathbb{Z}_2$ . The number of symmetry-related branches is equal to  $2 \times 7$ . Therefore, there are two such branches per equilibrium.

There is a symmetry-breaking from the planar families to solutions with isotropy group

$$\mathbb{Z}_2(\kappa_z). \quad (6)$$

These solutions have vertical component  $z = 0$ . In this case the  $\kappa_y$ -symmetry is broken, so these planar orbits are asymmetric with respect to the transformation that takes  $y$  to  $-y$ . Such solutions are observed for the third bifurcating family along  $L_2$  and the fourth family that bifurcates from  $L_1$ ; see Figure 4.

The Halo families  $H_1$  and  $H_2$  bifurcate from the Lyapunov families  $L_1$  and  $L_2$ , respectively. Each of these has isotropy group

$$\mathbb{Z}_2(\kappa_y), \quad (7)$$

*i.e.*, their solutions have the property that  $x(t)$  is even and  $y(t)$  is odd. Thus these spatial orbits are invariant under the transformation that takes  $y$  to  $-y$ .

The Axial families  $A_j$ , and similarly families  $B_j$ , bifurcate from  $V_j$ , for  $j = 1, 2, 3$ . Here the symmetry-breaking is from the group  $G_{V_j}$  to the group

$$\mathbb{Z}_2(\pi\kappa_y, \kappa_z). \quad (8)$$

This means that the Axial solutions satisfy  $\mathbf{u}(t) = R_z R_y(-t + \pi)$  or, setting  $\tilde{\mathbf{u}}(t) = \mathbf{u}(t + \pi/2)$ , that

$$\tilde{\mathbf{u}}(t) = R_z R_y \tilde{\mathbf{u}}(-t).$$

Then  $x(t)$  is even, and  $y(t)$  and  $z(t)$  are odd. Therefore these spatial orbits are invariant under the transformation that takes  $(y, z)$  to  $(-y, -z)$ .

## 5 Tertiary families

Tertiary symmetry-broken families (the green lines in Figure 2) correspond to families that bifurcate from solutions with isotropy groups (6), (7), and (8). Since these groups are isomorphic to  $\mathbb{Z}_2$ , the tertiary symmetry-broken solutions have the trivial isotropy group. Therefore, the number of symmetry-related branches of the tertiary families is  $4 \times 7$ , i.e. four per equilibrium. In particular, the symmetry-breaking bifurcations along the families  $A_3$  and  $B_3$  give rise to families that generate invariant surfaces.

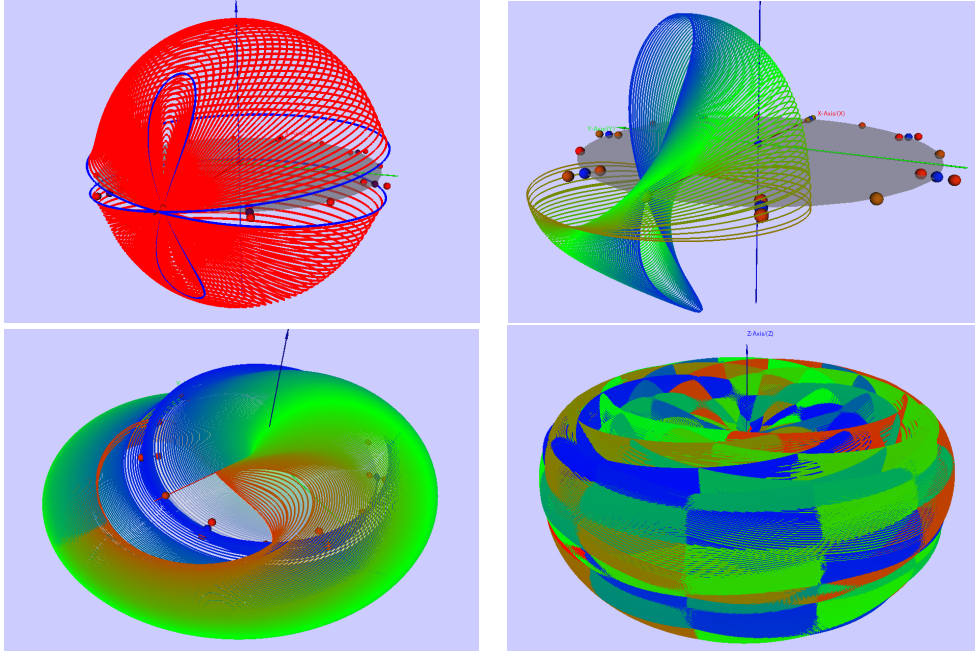


**Fig. 6.** Top Left: The Vertical family  $V_3$ , from the libration point  $\mathcal{L}_3$  until its second bifurcation orbit, with the bifurcation orbits colored blue. Top Right: The Axial family  $A_3$ , from the orbit it shares with  $V_3$  and until the orbit it shares with the planar family  $P_3$ . Bottom Left: The family  $B_3$ , from the orbit it shares with  $V_3$  and until the orbit it shares with the planar family  $P_3$ . Bottom Right: One of several families that bifurcate from  $B_3$ . The orbits of this family generate a torus that closes up after making two full rounds around the  $z$ -axis.

Indeed, the surface generated by the  $A_{3,1}$  family in Figure 5 reconnects to  $A_3$  after a complete loop around the central body, but to an orbit that is symmetric to the original one. Following this surface, i.e., its orbits, for a second loop around the central body, we obtain a double surface that interconnects the 7 pairs of Axial

bifurcation orbits that emanate from each of the 7 libration points symmetry-related to  $\mathcal{L}_3$ . The surface generated by the orbits of the family  $A_{3,1}$  contains an additional  $2 \times 7$  bifurcation orbits that connect to Halo families  $H_2$ . Consequently there is a continuous path in the bifurcation diagram between any of the 7 symmetry-related libration points  $\mathcal{L}_2$  and  $\mathcal{L}_3$ .

The surface generated by the orbits of the family  $A_{3,2}$  in Figure 5 is similar to that of  $A_{3,1}$  in that it interconnects  $2 \times 7$  bifurcation orbits along the Axial families  $A_3$ . These bifurcation orbits are distinct from the bifurcation orbits along  $A_3$  that are interconnected via the family  $A_{3,1}$ . The family  $A_{3,2}$  has  $2 \times 7$  extra bifurcation orbits that connect to Halo-like families that we do not describe here.

Several families bifurcate from the family  $B_3$  with trivial isotropy group, one of which is illustrated in the bottom right panel of Figure 6. This family is similar to  $A_{3,1}$  and  $A_{3,2}$  in that it connects one Axial family, with isotropy group  $\mathbb{Z}_2(\pi\kappa_y, \kappa_z)$ , to one Halo-like family, with isotropy group  $\mathbb{Z}_2(\kappa_z)$ . In future work we will report other families bifurcating from  $B_3$  that connect two Axial-like families with isotropy group  $\mathbb{Z}_2(\pi\kappa_y, \kappa_z)$ .

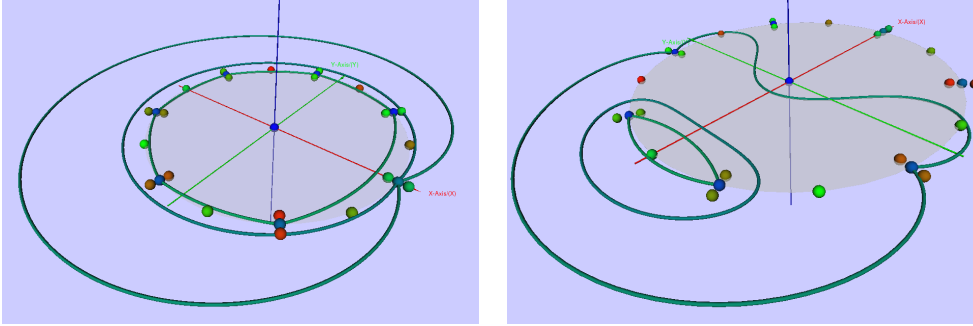


**Fig. 7.** Left: Three orbits from the planar, interplanetary family  $C_2$  from which the vertical family  $V_2$  bifurcates via a period-doubling. Right: Three orbits from the planar, interplanetary family  $P_3$  that bifurcates from the Axial family  $A_3$ .

## 6 Interplanetary orbits

Several families connect to planar families that encompass more than one body and that do not correspond to a planar Lyapunov family. Such families are referred to as interplanetary in [6], and indicated by black lines in the bifurcation diagram of Figure 2.

The family  $V_2$  has the symmetry group (5) and connects to a planar family  $C_2$  in Figure 7 via a reverse period-doubling bifurcation, *i.e.*, the vertical family  $V_2$  arises from the planar family via a period-doubling bifurcation. Indeed, the family  $V_2$  bifurcates from the interplanetary family  $C_2$  with isotropy group

$$\mathbb{Z}_2(\pi) \times \mathbb{Z}_2(\kappa_y) \times \mathbb{Z}_2(\kappa_z). \quad (9)$$

These planar solutions are  $\pi$ -periodic and their orbits are invariant under the transformation that takes  $y$  to  $-y$ . This is consistent with the symmetry-breaking phenomenon, since the isotropy group (5) is contained in the isotropy group of the interplanetary orbits (9).

The Lyapunov families  $V_1$  and  $V_3$  also connect to planar interplanetary families,  $C_1$  and  $C_3$ , respectively, via a period-doubling bifurcation. Actually,  $C_1$  and  $C_3$  correspond to the same family, *i.e.*,  $C_1 = C_3$ , and moreover, both  $V_1$  and  $V_3$  bifurcate from exactly the same orbit along  $C_1 = C_3$ , via a degenerate period-doubling bifurcation with two Floquet multipliers at  $-1$ .

Another family that ends in an interplanetary family is  $A_3$ ; see Figure 7. Here the isotropy group of the planar family  $P_3$  is

$$\mathbb{Z}_2(\pi\kappa_y) \times \mathbb{Z}_2(\kappa_z).$$

These solutions have the property that  $x(t)$  is even,  $y(t)$  is odd, and  $z = 0$ , so that the orbits are planar and symmetric with respect to the transformation that takes  $y$  to  $-y$ . Therefore the Axial family  $A_3$ , with group  $\mathbb{Z}_2(\pi\kappa_y, \kappa_z)$ , corresponds to a symmetry-breaking from the interplanetary family  $P_3$ .

**Acknowledgements.** We thank Ramiro Chavez Tovar for his assistance in producing the bifurcation diagram.

## References

1. D. Bang, B. Elmabsout, *Restricted  $n+1$ -body problem: existence and stability of relative equilibria*. Celestial Mechanics and Dynamical Astronomy, 89(4):305–318 (2004)
2. R. Calleja, E. Doedel, A. Humphries, A. Lemus-Rodríguez, B. Oldeman, *Boundary-value problem formulations for computing invariant manifolds and connecting orbits in the circular restricted three-body problem*. Celestial Mechanics and Dynamical Astronomy, 114(1-2):77-106 (2012)
3. C. García-Azpeitia, J. Ize, *Global bifurcation of planar and spatial periodic solutions in the restricted  $n$ -body problem*. Celestial Mechanics and Dynamical Astronomy, 110, 217-227 (2011)
4. C. García-Azpeitia, J. Ize, *Global bifurcation of planar and spatial periodic solutions from the polygonal relative equilibria for the  $n$ -body problem*. J. Differential Equations, 254(5), 2033–2075 (2013)
5. J. Henrard, *The web of periodic orbits at  $L_4$* . Modern celestial mechanics: from theory to applications (Rome, 2001). Celestial Mech. Dynam. Astronom. 83(1), 291–302 (2002).
6. T. J. Kalvouridis, *Particle motions in Maxwell's ring dynamical systems*. Celestial Mechanics and Dynamical Astronomy, 102(1-3):191–206 (2008)
7. J. Llibre, R. Martínez, C. Simó, *Transversality of the invariant manifolds associated to the Lyapunov family of periodic orbits near  $L_2$  in the restricted three-body problem*. J. Differ. Equations, 58, 104–156 (1985)
8. W. Koon, M. Lo, J. Marsden, S. Ross, *Heteroclinic connections between periodic orbits and resonance transitions in celestial mechanics*. Chaos. 10(2):427-469, (2000)
9. J. C. Maxwell. On the stability of motions of Saturn's rings. Macmillan and Co., Cambridge, 1859.
10. R. Moeckel, *Linear stability of relative equilibria with a dominant mass*. J. Dynam. Differential Equations, 6(1) (1994).
11. R. J. Vanderbei, E. Kolemen, *Linear stability of ring systems*, 133:656–664, (2007)
12. André Vanderbauwhede. *Branching of Periodic Orbits in Hamiltonian and Reversible Systems*. Equadiff 9: Proceedings of the 9th conference, Brno, 1997. pp. 169-181.
13. G. E. Roberts, *Linear stability in the  $1+n$ -gon relative equilibrium*. In J. Delgado, editor, Hamiltonian Systems and Celestial Mechanics. HAMSYS-98. World Sci. Monogr. Ser. Math. 6, 303–330. World Scientific (2000)
14. E. J. Doedel, R. C. Paffenroth, H. B. Keller, D. J. Dichmann, J. Galán-Vioque, A. Vanderbauwhede, *Continuation of periodic solutions in conservative systems with application to the 3-body problem*. Int. J. Bifurcation Chaos Appl. Sci. Eng. 13, 1–29 (2003)